Unified Approach to Pionization Structure

R. Michael Barnett and D. Silverman*
University of California, Irvine, California 92664
(Received 19 March 1973)

A unified treatment of peripheral models for the inclusive $q_\perp^2$ spectrum in the central plateau region is presented. The $q_\perp^2$ spectrum is calculated from several models of damping in internal momentum transfer. The highest-energy CERN Intersecting Storage Rings data for $p+p\rightarrow\pi+X$ is fitted for all $q_\perp$ by a power-law internal damping.

I. INTRODUCTION

The recent experiments at the CERN Intersecting Storage Rings (ISR) have confirmed the existence of a central plateau in the inclusive single-particle spectrum[1] and have found the $q_\perp^2$ dependence over a large region.[2] Different theoretical models have been used to account for different regions of the pionization data.[3-7] In this work we unify the treatment of these models by considering a general dynamical structure which includes all of these models as special cases and obeys the correct analyticity properties. It will be shown how specific forms for internal damping in momentum transfer lead directly to types of damping in $q_\perp^2$. We use one such form to obtain a fit to the $q_\perp$ dependence over the entire range of data at the highest ISR energy.

A theory for multiparticle production which describes the pionization or flat central plateau region must have a peripheral structure in order to decouple the detected particle c from the momentum and nature of the incoming particles in the central region of the inclusive single-particle spectrum, $a+b\rightarrow c+X$. This is indicated in Fig. 1, where the particle c is peripherally attached to the faster particles on the left-hand side and the slower particles on the right-hand side. A more general case is to peripherally produce a resonance or finite-mass fireball, and this will be considered in another paper.[8]

In order to obtain an asymptotic behavior as $s\rightarrow\infty$, we assume Regge behavior of the inclusive sums and phase-space integrals over the undetected particles $s_1^{\alpha_1(0)}$, $s_2^{\alpha_2(0)}$. The absolute-square and phase-space integration over this production amplitude gives the single-particle spectrum or the $M^2=(p_a+p_b+p_{\bar c})^2$ absorptive part of the forward 3 - 3 amplitude for $a+b+\bar{c}$ scattering (Fig. 2). The inclusive Regge behavior of s_1 and s_2 reappears as Regge behavior in energies s_l, s_r and gives the Mueller[9] double-Regge structure in the 3 - 3 amplitude, Fig. 3.

In order to get the pionization spectrum which shows rapid damping in $q_\perp$, we must add to this general structure some form for the damping of the internal momentum transfers t_l, t_r. The various models[3-7] for the pionization spectrum differ mainly in the assumed form for these momentum transfers as well as in the theoretical nature of the exchanged object. We will present a unifying formulation for computing the pionization spectrum from Fig. 2 with any internal-damping functions $\beta_l(t_l)$ and $\beta_r(t_r)$. It will be shown that the above formulation is sufficient to fit all of the highest-energy ISR pionization data with a single form for $\beta(t)$.

Previously, the single-particle spectrum from Fig. 1 or Fig. 2 has been calculated in the $s\rightarrow\infty$ limit for exponential damping in momentum transfer[5,6]

$$\beta_l(t_l)=e^{\Omega_l t_l},$$
$$\beta_r(t_r)=e^{\Omega_r t_r},$$

and gives a closed form for the result, Eq. (3.4). The square of any other internal damping $\beta(t)$ which is nonsingular and which vanishes for $t\rightarrow-\infty$, can be represented as a superposition of these exponentials:

$$A_r(t_r)\equiv\beta_r^2(t_r)=\int_0^\infty B_r(\Omega_r)\,e^{2\Omega_r t_r}\,d\Omega_r\;.$$

The result of calculating Fig. 2 for any such A_l, A_r will be a superposition over Ω_l, Ω_r of the results for the simple exponentials.

The general result, Eq. (2.11), agrees with the general analytic representation found by Zakrzewski[10] on the basis of analyticity arguments alone, since the diagram in Fig. 2 possesses the correct analyticity consistent with double-Regge behavior and has no simultaneous discontinuities in the overlapping variables s_l and s_r (Steinmann relations). Our derivation provides the physical meaning of the arbitrary weight function in this representation in terms of the internal damping functions $\beta(t)$.

Because of the generality of the formulation, it

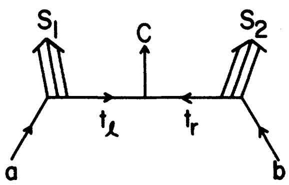

FIG. 1. Peripheral production amplitude for the central plateau region of the single-particle spectrum.

includes several physical models such as the exponential damping model of the small-$q_\perp$ region[4-6] and the power-law[3] or parton models[7] in the large-$q_\perp$ region. In this paper we show how to generate the phenomenologically proposed behaviors such as

$$e^{-a q_\perp^2}, \quad e^{-b q_\perp}, \quad (q_\perp)^{-n},$$

but the method outlined above modifies these to include the correct analytic behavior.

We have also treated the theory where the peripherally produced object is a spinless resonance which decays into two pions.[8] The large-transverse-momentum behavior of the resonance production reappears in the decay pion distribution modified at most by a power. A simple Amati-Fubini-Stanghellini (AFS) model with the only internal damping coming from pion propagators will be shown to give much too slow a power-law falloff.

In Sec. II we calculate the pionization spectrum for an arbitrary internal-damping function by expressing it in terms of its Laplace components and using the previously known phase-space integral over these components. In Sec. III we calculate in this formalism the pionization spectrum for the following specific models of internal damping: exponential in t, exponential in $(-t)^{1/2}$, and power law in t. We also discuss the results of the dual resonance model and summarize all of our results. The pionization data are fitted in Sec. IV with a specific power-law internal damping.

II. LAPLACE-TRANSFORM CALCULATION OF THE PIONIZATION SPECTRUM

The pionization spectrum may be computed from Fig. 1 or Fig. 2 as integrals over the momenta P_1 and P_2 of the inclusive sums:

$$\frac{d\sigma}{d^3q/E} = \frac{\lambda'}{s}\int d^4P_1\, d^4P_2\, \delta^4(P_1 + P_2 + q - p_a - p_b)\,\mathfrak{A}, \tag{2.1}$$

where q is the momentum of particle c and λ' is on over-all constant.

The term $\mathfrak{A}$ includes the inclusive sums and phase-space integrations that give rise to Regge behavior and is given in terms of the internal-damping functions $\beta(t)$:

$$\mathfrak{A} = \beta_l^{\,2}(t_l)\beta_r^{\,2}(t_r)(s_1)^{\alpha_1}(s_2)^{\alpha_2}, \tag{2.2}$$

where

$$\alpha_1 = \alpha_1(0), \quad \alpha_2 = \alpha_2(0).$$

This integration has been performed analytically for exponential internal damping functions.[5,6] We can easily extend this since any $\beta^2(t)$ that vanishes as $t \to -\infty$ can be expressed as a superposition of exponentials (a Laplace transform):

$$A_l(t_l) \equiv \beta_l^{\,2}(t_l) = \int_0^\infty d\Omega_l B_l(\Omega_l) e^{2\Omega_l t_l},$$
$$A_r(t_r) \equiv \beta_r^{\,2}(t_r) = \int_0^\infty d\Omega_r B_r(\Omega_r) e^{2\Omega_r t_r}. \tag{2.3}$$

This gives in (2.1)

$$\frac{d\sigma}{d^2q_\perp dy} = \frac{\lambda'}{s}\int_0^\infty d\Omega_l \int_0^\infty d\Omega_r\, B_l(\Omega_l)B_r(\Omega_r)\left[\int d^4P_1\, d^4P_2\,\delta^4(P_1+P_2+q-p_a-p_b)\, s_1^{\alpha_1} s_2^{\alpha_2}\exp(2\Omega_l t_l + 2\Omega_r t_r)\right]. \tag{2.4}$$

The integration in the square brackets has been performed in Refs. 5 and 6 and gives in the limit $s_l, s_r, s \to \infty$ in the pionization region with $m^2 = q^2$,

$$\frac{d\sigma}{d^2q_\perp dy} = \frac{\lambda'}{s}\int_0^\infty d\Omega_l \int_0^\infty d\Omega_r\, B_l(\Omega_l)B_r(\Omega_r)\pi\,\frac{\Gamma(\alpha_1+1)\Gamma(\alpha_2+1)}{8(\Omega_l+\Omega_r)^{\alpha_1+\alpha_2+2}}(\Omega_r s_l)^{\alpha_1}(\Omega_l s_r)^{\alpha_2}$$
$$\times \exp\left(\frac{2\Omega_l\Omega_r}{\Omega_l+\Omega_r}m^2\right)e^{-\kappa}\kappa^{-\alpha_1}\Psi(\alpha_2+1, -\alpha_1+\alpha_2+1;\kappa). \tag{2.5}$$

Ψ is the confluent hypergeometric function and

$$\kappa = \frac{2\Omega_l\Omega_r}{\Omega_l+\Omega_r}\eta, \tag{2.6}$$

$$\eta \equiv q_\perp^2 + m^2 = \frac{s_l s_r}{s}. \tag{2.7}$$

For the asymptotic energy limit we take α_1 and α_2 to be Pomeranchukon trajectories of unit intercept. This gives the single-particle spectrum from (2.5):

$$\frac{d\sigma}{d^2q_\perp dy} = \lambda \int_0^\infty d\Omega_l \int_0^\infty d\Omega_r\, B_l(\Omega_l) B_r(\Omega_r)(\Omega_l + \Omega_r)^{-3} \exp\left(\frac{2\Omega_l\Omega_r}{\Omega_l + \Omega_r} m^2\right) e^{-\kappa}\Psi(2, 1; \kappa). \tag{2.8}$$

This may also be rewritten using the relation[11]

$$e^{-\kappa}\Psi(2, 1, \kappa) = (1+\kappa)E_1(\kappa) - e^{-\kappa}, \tag{2.9}$$

where $E_1(\kappa)$ is the exponential integral function. Equation (2.8) is seen to be the result for internal exponential damping $e^{2\Omega_l t_l + 2\Omega_r t_r}$ obtained previously,[5] but now including a superposition over many different damping constants Ω_l, Ω_r with arbitrary amplitudes $B_l(\Omega_l)$, $B_r(\Omega_r)$.

The $q_\perp^2$ or η dependence of (2.8) occurs only in the variable κ, which depends on Ω_l, Ω_r only in the ratio

$$\Omega \equiv \frac{2\Omega_l\Omega_r}{\Omega_l + \Omega_r}. \tag{2.10}$$

It is then possible to express the $q_\perp^2$ dependence in a single integral over Ω by introducing into (2.8)

$$1 = \int_0^\infty d\Omega\, \delta\left(\Omega - \frac{2\Omega_l\Omega_r}{\Omega_l + \Omega_r}\right).$$

This gives in the pionization region the single integral representation

$$\frac{1}{\lambda}\frac{d\sigma}{d^2q_\perp dy} \equiv D(\eta) = \int_0^\infty d\Omega\, C(\Omega) e^{-\Omega\eta}\Psi(2, 1; \Omega\eta), \tag{2.11}$$

where

$$C(\Omega) = \int_0^\infty d\Omega_l \int_0^\infty d\Omega_r \delta\left(\Omega - \frac{2\Omega_l\Omega_r}{\Omega_l + \Omega_r}\right) B_l(\Omega_l) B_r(\Omega_r) \times (\Omega_l + \Omega_r)^{-3} e^{\Omega m^2}. \tag{2.12}$$

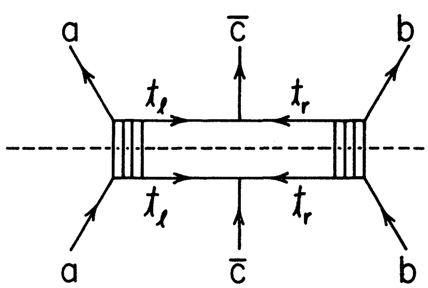

FIG. 2. Inclusive single-particle cross section as an absorptive part in $M^2 = (p_a + p_b + p_{\bar{c}})^2$ of forward $a + b + \bar{c}$ scattering.

The representation (2.11) [or more generally, a similar one derived from (2.5)] has been found by Zakrzewski[10] on the basis of analyticity requirements that include Regge behavior and absence of simultaneous singularities in the overlapping variables s_l, s_r. Our derivation connects the representation function $C(\Omega)$ with the dynamics of internal damping through (2.12) and (2.3).

A convenient form for calculating (2.12) is obtained by using

$$\tau_l \equiv \frac{1}{2\Omega_l}, \quad \tau_r \equiv \frac{1}{2\Omega_r}, \quad \tau_l + \tau_r = \frac{1}{\Omega}, \tag{2.13}$$

which gives

$$C(\Omega) = 16\Omega e^{m^2\Omega} \int_0^{\Omega^{-1}} d\tau_l \tau_l (\Omega^{-1} - \tau_l) \times B_l\left(\frac{1}{2\tau_l}\right) B_r\left(\frac{1}{2(\Omega^{-1} - \tau_l)}\right). \tag{2.14}$$

III. SPECIFIC MODELS OF INTERNAL DAMPING

In this section we apply the general result to the calculations of the spectrum resulting from specific choices of $\beta(t)$ which correspond to some current models.

A. Exponential Damped Model

Motivated by exponential damping in exclusive momentum transfers, Caneschi and Pignotti[4] and Silverman and Tan[5] used single exponentials to calculate the spectrum. In our formalism this becomes simply:

$$\beta_l(t_l) = e^{a_l t_l}, \quad \beta_r(t_r) = e^{a_r t_r}, \tag{3.1}$$

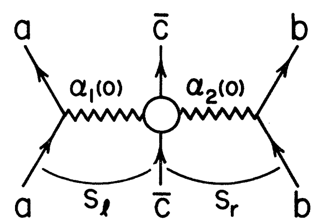

FIG. 3. Double-Regge behavior in forward $a + b + \bar{c}$ resulting from inclusive Regge behavior in Fig. 2.

$$B_l(\Omega_l)=\delta(\Omega_l-a_l),\quad B_r(\Omega_r)=\delta(\Omega_r-a_r), \tag{3.2}$$

$$C(\Omega)=\delta\left(\Omega-2\frac{a_l a_r}{a_l+a_r}\right)(a_l+a_r)^{-3}e^{\Omega m^2}, \tag{3.3}$$

$$D(\eta)=e^{-a\eta}\Psi(2,1;a\eta), \tag{3.4}$$

where

$$a\equiv\frac{2a_l a_r}{a_l+a_r}.$$

As $\eta\to\infty$,

$$D(\eta)\sim\frac{e^{-a\eta}}{\eta^2}\times\text{const}. \tag{3.5}$$

B. Exponential Damped in $(-t)^{1/2}$

Since the maximum possible falloff of a form factor is $e^{-a(-t)^{1/2}}$, and the small-momentum-transfer spectrum follows a behavior $e^{-ap_\perp}$, we study the case

$$\beta_l(t)=\beta_r(t)=e^{-a(-t)^{1/2}},$$
$$B(\Omega_l)=\left(\frac{a^2}{2\pi}\right)^{1/2}\Omega_l^{-3/2}\exp\left(-\frac{a^2}{2\Omega_l}\right). \tag{3.6}$$

This gives

$$C(\Omega)=\tfrac{5}{16}a^2\Omega^{-5}\exp\left(m^2\Omega-\frac{a^2}{\Omega}\right). \tag{3.7}$$

For large η, we can find from the integral representation (2.11) that

$$D(\eta)\sim10(\tfrac{1}{2}\pi)^{1/2}a^{-9/2}\eta^{3/4}e^{-a\sqrt{\eta}}. \tag{3.8}$$

C. Power-Law Damping

This case is motivated by the power-law falloff of the large-$q_\perp$ pionization data, as well as by the power-law behavior of propagators and form factors. This includes the most simple AFS model of pion exchanges producing ρ's. It also includes the parton models of the large-transverse-momentum region.[7]

We parametrize the internal damping with respect to an effective mass squared μ^2:

$$\beta_l(t)=\beta_r(t)=\frac{1}{(t-\mu^2)^\gamma}, \tag{3.9}$$

$$A_l(t)=A_r(t)=\frac{1}{(t-\mu^2)^{2\gamma}}, \tag{3.10}$$

$$B(\Omega_l)=\frac{4^\gamma}{\Gamma(2\gamma)}\Omega_l^{2\gamma-1}e^{-2\mu^2\Omega_l}, \tag{3.11}$$

$$C(\Omega)=\frac{32\pi^{1/2}}{[\Gamma(2\gamma)]^2}\left(\frac{\mu^2}{4}\right)^{1-\gamma}e^{\Omega m^2}\Omega^{3\gamma-3}e^{-2\mu^2\Omega}\times W_{\gamma-3/2,3/2-\gamma}(4\mu^2\Omega), \tag{3.12}$$

where $W_{\lambda,\nu}$ is a Whittaker function.[12]

If the produced particle is a pion, we may take $m_\pi^2\approx0$ and for $\gamma>\frac{3}{4}$, we obtain $D(\eta)$ in terms of a Meijer G function[13] (see Appendix A):

$$D(\eta)=\frac{\text{const}}{\eta^{2\gamma}}G_{33}^{22}\left(4\mu^2/\eta\,\middle|\,\begin{matrix}1-2\gamma & 1-2\gamma & \frac{1}{2}\\ 0 & -3+2\gamma & -1-2\gamma\end{matrix}\right). \tag{3.13}$$

The asymptotic behavior of $D(\eta)$ can be obtained from (3.12) in the integral representation (2.11) or from (3.13) (see Appendix A). As $\eta\to\infty$, the integral (2.11) is damped by $e^{-\Omega\eta}$ so that the important Ω are $\Omega\to0$. In this limit,

$$C(\Omega)\sim\text{const}\times\Omega^{2\gamma-1}+\text{const}\times\Omega^{4\gamma-4}. \tag{3.14}$$

Scaling the integration variable to $x=\Omega\eta$ gives the results

$$D(\eta)\sim\eta^{3-4\gamma},\quad \tfrac{3}{4}<\gamma\leq\tfrac{3}{2},$$
$$D(\eta)\sim\eta^{-2\gamma},\quad \tfrac{3}{2}<\gamma. \tag{3.15}$$

As $\eta\to0$, the integral inherits the logarithmic η branch point in

$$\Psi(2,1;\Omega\eta)\underset{\Omega\eta\to0}{\sim}-\ln(\Omega\eta) \tag{3.16}$$

and is damped by $e^{-(4\mu^2-m^2)\Omega}$ if $4\mu^2-m^2>0$. In this case

$$D(\eta)\underset{\eta\to0}{\sim}-\ln\eta. \tag{3.17}$$

If $m^2-4\mu^2>0$, however, there is a branch point at $\eta=m^2-4\mu^2$. In either case the singularities are outside the physical region since $\eta=q_\perp^2+m^2$. For the case of ρ production with pion exchange and only the pion propagators giving damping we have $\gamma=1$ and the ρ's are transversely damped in terms of

$$\eta_\rho\equiv(q_\rho^\perp)^2+m_\rho^2,$$

so that

$$D(\eta_\rho)\underset{\eta_\rho\to\infty}{\sim}1/\eta_\rho.$$

In Ref. 8 we show that this leads to a spectrum for the decay pions of

$$D(\eta)\underset{\eta\to\infty}{\sim}\frac{1}{\eta}. \tag{3.18}$$

D. Dual-Resonance-Model Tree Diagram

Although the dual-resonance-model tree diagrams do not contain an internal structure as in Fig. 2, the 3-3 amplitude has an M^2 absorptive part.[14] Since it also has Regge behavior and the absence of singularities in overlapping variables,[15] it falls into the representation (2.11).[10] With α' the trajectory slope, the M^2 absorptive part is given by (2.11) with

$$C(\Omega)=\Omega^{-3/2}(\Omega-4\alpha')^{-1/2}\theta(\Omega-4\alpha') \tag{3.19}$$

and

$$D(\eta)=\eta e^{-4\alpha'\eta}\Psi(\tfrac{1}{2},4;4\alpha'\eta)\,. \tag{3.20}$$

For large η,

$$D(\eta)\underset{\eta\to\infty}{\sim}\eta^{1/2}e^{-4\alpha'\eta}\,,$$

resembling the exponential-damping result.

E. Summary

The large-η behavior of the examples in Secs. III A, III B, and III C lead us to the following recipe for finding an internal damping which will yield a desired large-η behavior: If the internal damping falls off faster than $(-t)^{-3/2}$ for large $|t|$, then the dominant damping for large η is the same as that for large $|t|$. Numerical studies also show that as $q_\perp{}^2$ approaches zero, the increase of $D(\eta)$ is much smaller than would be obtained by using only the associated asymptotic forms

$$e^{-aq_\perp{}^2},\quad e^{-bq_\perp},\quad (q_\perp{}^2)^{-\gamma}\,,$$

respectively.

IV. COMPARISON WITH PIONIZATION SPECTRUM DATA

We have studied three general $q_\perp$ behaviors: $\sim e^{-aq_\perp{}^2}$, $\sim e^{-bq_\perp}$, $\sim(q_\perp{}^2)^{-\gamma}$. These will now be compared with the highest-energy ISR spectrum for $p+p\to\pi+X$ in the pionization region.[2]

The region of $0.2\le q_\perp\le 0.8$ can be fitted with the internal exponential damping form of Sec. III A with $a=2.7\ \text{GeV}^{-2}$. The region $0.2\le q_\perp\le 1.1$ can be fitted with the $e^{-b(-t)^{1/2}}$ internal damping form of Sec. III B. However, both of these fits fall off too fast in $q_\perp$ to fit higher-$q_\perp$ data. To study the power-law damping form, we plot in Fig. 4 the data for $\ln(d\sigma/d^2q_\perp dy)$ vs $\ln(\eta)=\ln(q_\perp{}^2+m_\pi{}^2)$. For large η the curve becomes linear with a slope indicating a large-$q_\perp$ power-law behavior like $q_\perp{}^{-8}$ or η^{-4}, as previously recognized by others.[7] From (3.15) we conclude that $\gamma=2$. This rules out the possibility of damping from single propagators only, which behaves like η^{-1} from (3.18).

We have used the internal power law damping of Sec. III C with $\gamma=2$,

$$\beta_l(t)=\beta_r(t)=(a^2-t)^{-2}\,,$$

to give the fit shown in Fig. 4 with the integral over $C(\Omega)$ in (3.12) calculated numerically. Using an effective mass $a=0.485$ GeV, the fit covers nine orders of magnitude of cross section.

ACKNOWLEDGMENT

We thank our colleagues at Irvine for helpful discussions.

APPENDIX A

We calculate the integral from Sec. III C for $m_\pi{}^2\approx 0$:

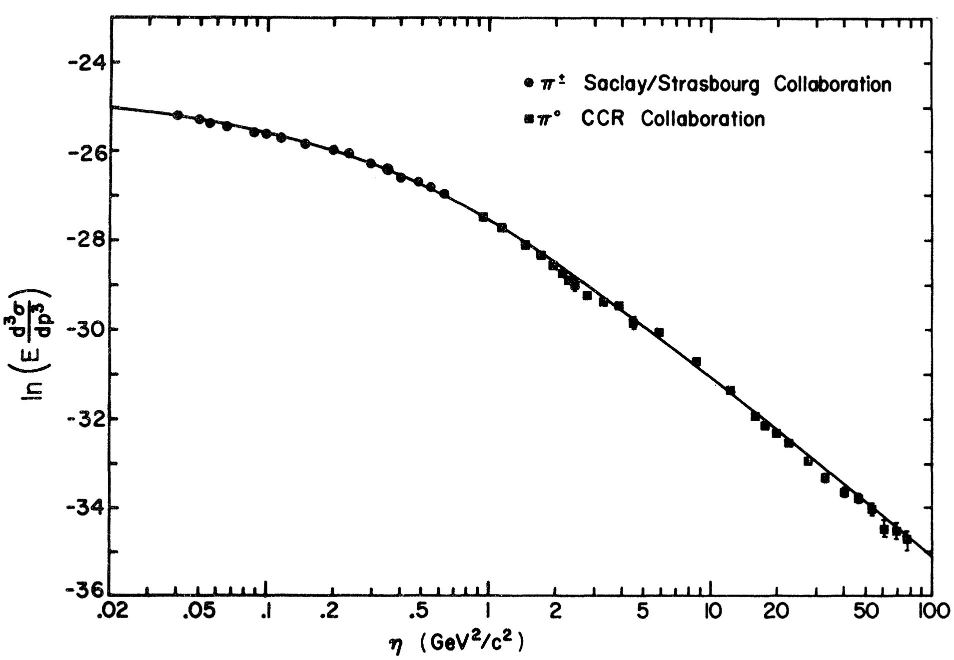

FIG. 4. Fit to the $s^{1/2}=53$ GeV/c ISR data for $p+p\to\pi+X$, using $\beta(t)=(t-a^2)^{-2}$ for power-law internal damping with $a=0.485$ GeV and $\eta=q_\perp{}^2+m_\pi{}^2$.

$$D(\eta)=\int_0^\infty d\Omega[\Omega^{3\gamma-3}\exp(-2\mu^2\Omega)W_{\gamma-3/2,3/2-\gamma}(4\mu^2\Omega)]\times e^{-\eta\Omega}\Psi(2,1;\eta\Omega)\,. \quad \text{(A1)}$$

We use the Mellin convolution theorem[16] (see Ref. 17):

$$\int_0^\infty dx\, v(x)w(x)=\frac{1}{2\pi i}\int_{-i\infty+\sigma}^{i\infty+\sigma}W_m(\rho)V_m(1-\rho)d\rho\,, \quad \text{(A2)}$$

where

$$W_m(\rho)\equiv\int_0^\infty d\Omega\, w(\Omega)\Omega^{\rho-1}\,. \quad \text{(A3)}$$

Regarding the bracketed expression in (A1) as $w(\Omega)$, we find from (A3) that

$$W_m(\rho)=(4\mu^2)^{3-3\gamma-\rho}\frac{\Gamma(\rho-1+2\gamma)\Gamma(\rho-4+4\gamma)}{\Gamma(\rho-\frac{1}{2}+2\gamma)}\,. \quad \text{(A4)}$$

Similarly,

$$V_m(1-\rho)=\int_0^\infty d\Omega\,\Omega^{-\rho}e^{\eta\Omega}\Psi(2,1;\eta\Omega)=\frac{1}{\eta^{1-\rho}}\frac{\Gamma(1-\rho)\Gamma(1-\rho)}{\Gamma(3-\rho)}\,. \quad \text{(A5)}$$

From (A1) and (A2) we now have

$$D(\eta)=\frac{(4\mu^2)^{3-3\gamma-\sigma}}{\eta^{1-\sigma}(2\pi i)}\int_{-i\infty}^{i\infty}d\rho\left(\frac{\eta}{4\mu^2}\right)^\rho\frac{\Gamma(1-\sigma-\rho)\Gamma(1-\sigma-\rho)\Gamma(2\gamma-1+\sigma+\rho)\Gamma(4\gamma-4+\sigma-\rho)}{\Gamma(2\gamma-\frac{1}{2}+\sigma+\rho)\Gamma(3-\sigma-\rho)}\,. \quad \text{(A6)}$$

There are three conditions on σ:

$$\sigma<1\,,\quad \sigma>1-2\gamma\,,\quad \sigma>4-4\gamma\,,$$

which can always be met if $\gamma>\frac{3}{4}$. For $\gamma>\frac{7}{8}$ we choose $\sigma=\frac{1}{2}$ and obtain the result

$$D(\eta)=\eta^{-1/2}(4\mu^2)^{5/2-3\gamma}\times G^{22}_{33}\left(\eta/4\mu^2\left|\begin{matrix}\frac{3}{2}-2\gamma & \frac{9}{2}-4\gamma & \frac{5}{2}\\ \frac{1}{2} & \frac{1}{2} & 1-2\gamma\end{matrix}\right.\right)\,, \quad \text{(A7)}$$

where G is a Meijer's G function.[13]

We will need three properties[13]:

$$Z^\sigma G^{22}_{33}\left(Z\left|\begin{matrix}a_1 & a_2 & a_3\\ b_1 & b_2 & b_3\end{matrix}\right.\right)=G^{22}_{33}\left(Z\left|\begin{matrix}a_1+\sigma & a_2+\sigma & a_3+\sigma\\ b_1+\sigma & b_2+\sigma & b_3+\sigma\end{matrix}\right.\right)\,, \quad \text{(A8)}$$

$$G^{22}_{33}\left(Z\left|\begin{matrix}a_1 & a_2 & a_3\\ b_1 & b_2 & b_3\end{matrix}\right.\right)=G^{22}_{33}\left(Z^{-1}\left|\begin{matrix}1-b_1 & 1-b_2 & 1-b_3\\ 1-a_1 & 1-a_2 & 1-a_3\end{matrix}\right.\right)\,, \quad \text{(A9)}$$

$$G^{22}_{33}\left(Z\left|\begin{matrix}a_1 & a_2 & a_3\\ b_1 & b_2 & b_3\end{matrix}\right.\right)\underset{Z\to 0}{=}O(Z^b)\,, \quad \text{(A10)}$$

where $b\equiv\min(b_1,b_2)$.

From (A8) and (A9) we get the form useful for large η and $\gamma>\frac{3}{4}$:

$$D(\eta)=\frac{(4\mu^2)^{2-\gamma}}{\eta^{2\gamma}}G^{22}_{33}\left(4\mu^2/\eta\left|\begin{matrix}1-2\gamma & 1-2\gamma & \frac{1}{2}\\ 0 & -3+2\gamma & -1-2\gamma\end{matrix}\right.\right)\,. \quad \text{(A11)}$$

From (A10), the asymptotic $\eta\to\infty$ behavior is dependent on γ, so that

$$\text{for } \gamma\geq\tfrac{3}{2},\ D(\eta)\underset{\eta\to\infty}{\sim}\frac{1}{\eta^{2\gamma}}\,, \quad \text{(A12)}$$

and

$$\text{for } \tfrac{3}{2}\geq\gamma\geq\tfrac{3}{4},\ D(\eta)\underset{\eta\to\infty}{\sim}\frac{1}{\eta^{4\gamma-3}}\,.$$

*Supported in part by the National Science Foundation.

[1]J. C. Sens, review talk, in *Proceedings of the Fourth International Conference on High Energy Collisions, Oxford, 1972,* edited by J. R. Smith (Rutherford High Energy Laboratory, Chilton, Didcot, Berkshire, England, 1972), p. 177.

[2]R. Cool *et al.* (CERN/Columbia/Rockefeller Collaboration), in *Proceedings of the Sixteenth International Conference on High Energy Physics, National Accelerator Laboratory, Batavia, Ill., 1972,* edited by J. D. Jackson and A. Roberts (NAL, Batavia, Ill., 1973); M. Banner *et al.* (Saclay/Strasbourg Collaboration), *ibid.*

[3]D. Amati, S. Fubini, and A. Stanghellini, Nuovo Cimento 26, 896 (1962).

[4]L. Caneschi and A. Pignotti, Phys. Rev. Lett. 22, 1219 (1969).

[5]D. Silverman and C.-I Tan, Nuovo Cimento 2A, 489 (1971).

[6]D. Silverman, this issue, Phys. Rev. D 8, 2279 (1973).

[7]S. M. Berman, J. D. Bjorken, and J. B. Kogut, Phys. Rev. D 4, 3388 (1971); J. F. Gunion, S. J. Brodsky, and R. Blankenbecler, Phys. Lett. 39B, 649 (1972); Phys. Rev. D 6, 2652 (1972); Phys. Lett. 42B, 461 (1972). P. V. Landshoff and J. C. Polkinghorne, DAMTP Report No. 72/43 and No. 72/48 (unpublished). D. Amati, L. Caneschi, and M. Testa, Phys. Lett. 43B, 186 (1973).

[8]R. M. Barnett and D. Silverman, University of California, Irvine, Report No. 73-15 (unpublished).

[9]A. H. Mueller, Phys. Rev. D 2, 2963 (1970).

[10]W. J. Zakrzewski, Phys. Lett. 40B, 645 (1972).

[11]C. H. Mehta and D. Silverman, Nucl. Phys. B52, 77 (1973).

[12]I. S. Gradshteyn and I. M. Ryzhik, *Table of Integrals,*

Series, and Products (Academic, New York, 1965), pp. 1059–1063.
[13]I. S. Gradshteyn and I. M. Ryzhik, *Table of Integrals, Series, and Products*, Ref. 12, pp. 1068–1071 (the conditions on the expansion on p. 1069 are in error); *Higher Transcendental Functions* (Bateman Manuscript Project), edited by A. Erdélyi (McGraw-Hill, New York, 1953), Vol. I, pp. 206–222; *Tables of Integral Transforms* (Bateman Manuscript Project), edited by A. Erdélyi (*ibid*), Vol. II, pp. 391–444; Yudell L. Luke, *The Special Functions and Their Approximations* (Academic, New York, 1969), pp. 136–234.
[14]C. E. DeTar, Kyungsik Kang, C.-I Tan, and J. H. Weis, Phys. Rev. D 4, 425 (1971).
[15]C. H. Mehta and D. Silverman, Nucl. Phys. (to be published).
[16]P. M. Morse and H. Feshbach, *Methods of Theoretical Physics* (McGraw-Hill, New York, 1953), Vol. I.
[17]Although the integral (A1) is given in Erdélyi, *Tables of Integral Transforms*, Vol. II (see Ref. 13), p. 411, Eq. 46, and is quoted in Gradshteyn, Eq. 7.625.3, the results given there are erroneous.

PHYSICAL REVIEW D VOLUME 8, NUMBER 7 1 OCTOBER 1973

Analytic Representation for Deep-Inelastic Electroproduction Structure Functions

H. K. Shepard and L. M. Simmons, Jr.
Department of Physics, University of New Hampshire, Durham, New Hampshire 03824
(Received 18 June 1973)

Conformal mapping and the ideas of analytic data analysis are used to obtain a new variable for the parametrization of the deep-inelastic proton scaling function, $F_2(\omega)$. The resulting fits to the scaling-region data are excellent. We note that present scaling data do not uniquely constrain the threshold behavior. Extrapolations to large ω favor a decreasing F_2. Assuming that a simple analytic continuation to the $e^+e^- \to \bar{p}\ X$ channel is allowed, the fits are extrapolated to this region. The extended reciprocal relation is also discussed.

I. INTRODUCTION

Experiments[1,2] on the inclusive reaction $e^- + p \to e^- + X$ ("anything") strongly support the scaling hypothesis of Bjorken,[3,4] that in the appropriate kinematic regime the structure functions depend on a single variable, ω. We have used the ω-plane analytic structure suggested by one reasonable field-theory model[5] (which gives Bjorken scaling) and constructed a new variable by conformal mapping. Power series in this variable provide excellent fits to the experimental data in the scaling region. We further consider extrapolations of our parametrizations to high ω and find that a decreasing $F_2(\omega)$ is favored. Assuming that the dynamics allow continuation to the annihilation channel, $e^+ + e^- \to \bar{p} + X$, we extrapolate our representations to this region of the ω plane and draw some limited conclusions. We also briefly discuss the Gribov-Lipatov[6,7] reciprocal relation.

In the remainder of this section we describe the kinematics for $e^- + p \to e^- + X$, shown in Fig. 1. Following standard usage,[4,7] we define $\nu = p\cdot q/M$, $W^2 = (p+q)^2$, $\omega = 1/x = -2M\nu/q^2$. In our metric $q^2 \leq 0$ and $\nu \geq 0$ for electroproduction; M is the nucleon mass (the electron mass is neglected). Since $W^2 \geq M^2$ it is easy to show that $1 \leq \omega < \infty$ for $e^-p \to e^-X$. (For $e^+e^- \to \bar{p}X$, $0 < \omega \leq 1$. See Sec. V.) The Bjorken scaling limit[3] is the kinematic region $|q^2| \to \infty$, ω fixed, $W^2 >> M^2$.

Assuming one-photon exchange, the cross section for inclusive electroproduction is described by two structure functions,[8] $W_1(q^2, \nu)$ and $W_2(q^2, \nu)$. Both W_1 and W_2 are non-negative in the physical ep scattering region. According to the scaling hypothesis, $W_1(q^2, \nu)$ and $\nu W_2(q^2, \nu)$ become functions of the single variable ω in the Bjorken limit. We thus define

$$F_1(\omega) \equiv \lim_{\substack{-q^2\to\infty \\ \omega \text{ fixed}}} [MW_1(q^2, \nu)],$$

$$F_2(\omega) \equiv \lim_{\substack{-q^2\to\infty \\ \omega \text{ fixed}}} [\nu W_2(q^2, \nu)].$$

In terms of the parameter $R = \sigma_s/\sigma_t$, the ratio of the photoabsorption cross sections for longitudinal and transverse virtual photons,[1,2] F_1 and F_2, are related by

$$F_1(\omega) = \tfrac{1}{2}(1+R)^{-1}\omega F_2(\omega) \tag{1.1}$$

in the scaling limit. Thus, if R is a constant (or a function of ω only), $F_1(\omega)$ automatically obeys the scaling hypothesis if $F_2(\omega)$ does. In Sec. III we shall assume R to be constant and thus only discuss fits to $F_2(\omega)$.